Ref. No. 0041 Abstract Category: 5.09

DESIGN AND FABRICATION OF A FORWARD VIEW SCANNER ON SIOB WITH LATCH STRUCTURE FOR IMPROVED VERTICAL ORIENTATION

Dingkang Wang[1], Dong Zheng[1], Sanjeev Koppal[1], Boqian Sun[2], and Huikai Xie[2]*
[1]Department of Electrical & Computer Engineering, University of Florida, Gainesville, Florida, USA
[2]School of Information and Electronics, Beijing Institute of Technology, Beijing, China

ABSTRACT

MEMS mirror based forward-view optical scanning typically requires a second mirror to direct the optical beam forward, which increases the size and weight of the scanner drastically. This paper reports a compact forward-view laser scanner with two vertically oriented scanning micromirrors integrated on a silicon optical bench. This concept was previously explored, but the bending angles of the vertical mirrors had large deviations (typically ±15°) from 90°. In this work, a new latch structure is proposed to secure the mirror frame at its vertical position and an array of meander thin-film stripes is proposed to ensure the latching. The new design has been successfully fabricated and shows much-improved verticality with a maximum deviation of less than ± 2° from 90°. The measured forward field of view (FoV) of the vertical micromirror reaches 20° in both axes at non-resonance with the voltage amplitude less than 3.5 V. The first-order resonant frequency of the micromirror is about 630 Hz. A forward scanning LiDAR has been built with this new MEMS scanner and 3D point clouds have been achieved.

KEYWORDS

MEMS mirror, LiDAR, electrothermal actuation, forward-scanning

INTRODUCTION

LiDAR (light detection and ranging) systems are powerful sensors for autonomous vehicles. Meanwhile, microrobots are also demanding the capability of LiDAR. However, conventional LiDAR are bulky and usually employ motorized scanners that are large with weights in the order of kg's, vulnerable to mechanical shocks and vibrations, and expensive [1]. Thus, miniaturization of LiDAR, especially the laser scanner, is needed.

Laser scanners based on MEMS mirrors are small and have been used to build compact LiDAR systems [1]-[7]. For example, Kasturi et al. demonstrated an electrostatic MEMS mirror based LiDAR with a small form factor of 90 mm × 60 mm × 40 mm and a light weight of 46 g [1]. Hofmann et al. reported large-aperture (7 mm in diameter) electrostatic MEMS mirrors for long-distance LiDAR [3]. Electromagnetic MEMS mirrors have also been developed, for instance by Ye et al. [4] and Periyasamy et al. [5], for LiDAR because of their advantages of wide angles and large mirror apertures. Generally, electrostatic MEMS mirrors need large areas for their comb drives while electromagnetic MEMS mirrors require large coils or magnets to generate the actuation force, so their fill factors are low (typically less than 5%). Jia et al. proposed a gimbal-less 2-axis electrothermal MEMS mirror with a fill factor of 25% using an inverted-series-connected (ISC) electrothermal bimorph actuator design [6]. Using this ISC actuator design, Wang et al. developed an electrothermal MEMS mirror based multi-functional LiDAR with the dimensions of 21 cm × 9 cm × 6.5 cm [7].

However, those MEMS-based LiDAR are still significantly oversized and overweighed for micro-air vehicles (MAVs). For example, the Robobee, an insect-like MAV developed by Baisch and Wood [8], weighs less than 0.1 g. One of the reasons laser scanners composed of small MEMS mirrors are still relatively large is often caused by the need of assembling an extra mirror to fold the laser beam to scan forward as forward-view detection is of high interest for almost all MAVs.

In order to eliminate the extra folding mirror, the authors proposed and demonstrated a compact forward-view MEMS laser scanner with two vertical MEMS mirrors integrated on one silicon optical bench (SiOB), which weighed only 20 mg [10]. This novel design significantly reduces the packaging size and assembling and alignment efforts. However, the vertical orientation angles of the MEMS mirrors had large deviations in the range of -27° to +10° from exactly 90° [10], which not only brings uncertainties to the forward scanning direction but also requires extra efforts or structures to adjust the scanning direction. Furthermore, the vertical micromirrors were held out of plane by arrays of bending bimorph beams. So, the mirror frames were not secured, significantly affecting the 2D scanning of the vertical micromirrors.

Therefore, in this work, a new latch structure, as illustrated in Figure 1(c), is proposed to lock and secure the mirror frame at 90°. This latch structure replaces the previous stopper structure on the SiOB and can lock the vertical position after the mirror frame is released. In addition, to guide the mirror frame into the latch, a group of pulling strings is designed on the mirror frame. The new SiOB based MEMS vertical micromirrors are successfully fabricated and exhibit much better verticality and much less coupling from the mirror frame. Finally, a LiDAR system based on this novel forward-view scanning MEMS mirror is built and point clouds are successfully generated.

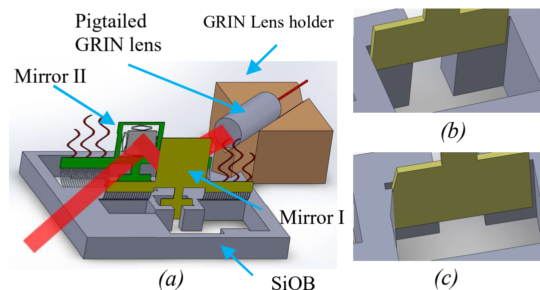

Figure 1. (a) A 3D model of the MEMS scanner with two vertical mirrors on a SiOB with a pigtailed GRIN lens on a lens holder. The stopper design for the previous works is (b), and (c) is the new latch design.

MEMS DESIGN

As illustrated in Figure 1(a), the proposed MEMS scanners have two vertically oriented micromirrors (Mirror I and Mirror II), which are both designed to stand upright on the SiOB. An alignment trench is designed on the SiOB to assist the alignment of the laser beam. The laser beam first reaches Mirror I. Then Mirror II folds the laser beam and scans the laser in the forward direction. Mirror I can be a non-scanning fixed mirror or a scanning mirror. Mirror II is always a 2-axis scanning micromirror.

Similar to the previous design, the vertical bending is achieved through Tungsten (W)/SiO_2 bimorph arrays [10]. The high residual stresses in the W/SiO_2 bimorph arrays generate the bending torque to pull-up the mirror frame, as shown in Figure 1(a). In a previous design [10], a stopper structure with an extension bar was implemented, as illustrated in Figure 2(a), in which ideally the stopper and the bar can stop the mirror frame at exactly 90° even when the bending bimorph beams try to pull the mirror frame to over 90°. However, fabrication variations always cause nonideal results. As shown by the SEMs of some fabricated devices in Figure 3, the silicon sidewalls are typically sloped from the etching process, so the mirror frame will be tilted even when the W/SiO_2 beams are over-stressed. When the W/SiO_2 beams are under-stressed, the tilt of the mirror frame may be quite large, as illustrated in Figure 2(c), and the radius of curvature of the W/SiO_2 bimorph array changing with the micromirror actuation voltage creates another scanning variation issue.

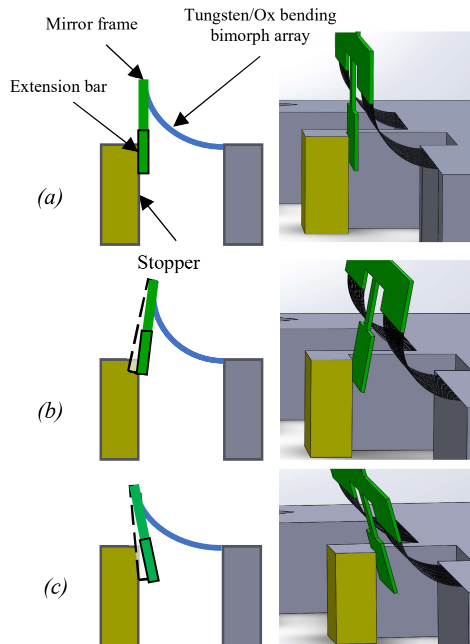

Figure 2. The problems of the previous stopper. (a) Ideal case. (b) If the W/SiO_2 beams are over-stressed, the tilt of the mirror frame will be larger than 90°. (c) If the W/SiO_2 beams are under-stressed, the tilt of the mirror frame will be smaller than 90°.

As shown in Figures 3, the bending angle of a previously fabricated micromirror was less than 90°, meaning that the residual stresses in the W/SiO_2 bimorph beams were not high enough. However, overly increasing the residual stress level always causes the W layer to peel off. Increasing the length of the bimorph beams can increase the bending angle without increasing the stress level, but this also reduces the stiffness of the bending bimorph beams, making the mirror frame even more susceptible to the environmental vibrations and variations.

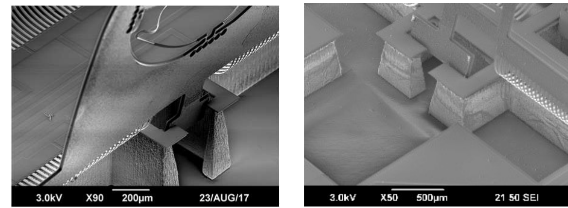

Figure 3. The SEMs of the stoppers in the previous works.

Considering all the deficiencies of the previous stopper design, a new latch design is proposed and illustrated in Figure 4(a). A mirror frame bar will fall into the latch structure, and the bending angle of the mirror frame will be fixed at 90°, as illustrated in Figure 4(b).

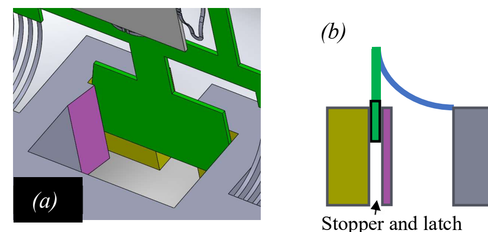

Figure 4 (a) Latch design. (b) The expected result of the latch structure.

The latch structure requires the bar of the mirror frame fits into the notch on the silicon substrate. The designed width of the notch is 10 µm wider than the thickness of the mirror frame (20 µm) to make sure the mirror frame bar can always fit into the notch. The estimated variation range is 90°±1.6° by considering the process variation.

Fitting the mirror frame bar into the notch is challenging. Thus, assistant pulling strings are designed to connect the mirror frame and the SiOB substrate, as shown in the layout in Figure 5. The pulling strings have two functions. First, it can help to slow down the unwanted silicon etching of the backside of the mirror plate during release. Second, the pulling strings can be used as an assistant structure to guide the mirror frame and fit the frame bar into the notch if the bar does not fall into the notch automatically, as illustrated in Figure 6. The layer structure of the pulling strings is a stack of 0.2 µm Pt, 1 µm Al and 1 µm SiO_2 to make sure they will not break easily during the release or being pulled.

The vertical micromirrors are electrothermally-actuated and based on the inverted-series-connected (ISC) bimorph actuation structure reported in [6]. The MEMS mirror has a footprint of 4.9 mm by 4.7 mm. The notch on the top-left of the SiOB is angled 45° to Mirror I. Mirror I is a non-scanning mirror with a size of 1.2 mm by 1.05 mm. Mirror II is a 2D scanning mirror with a size of 0.68 mm by 0.6 mm. Mirror I and Mirror II are bent by 42 and 44 W/SiO_2 bending bimorph beams, respectively.

FABRICATION AND RELEASE

The device fabrication starts with an SOI wafer whose device layer is 20 µm thick, which defines the thicknesses of the mirror plates and the vertical mirror frames. The SOI handle layer thickness is 500 µm. The fabrication process flow is similar to the one reported in [10].

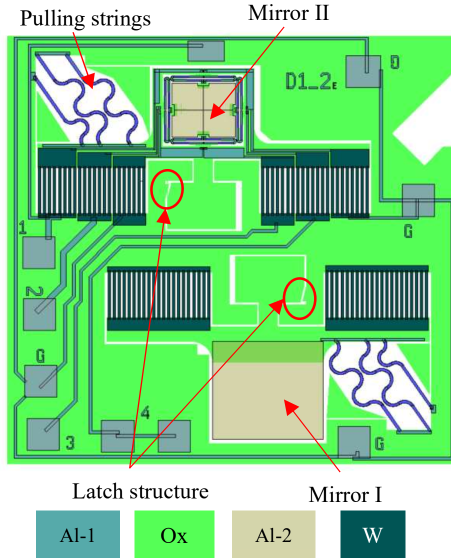

Figure 5. Proposed device topology with the latch structure and the pulling strings.

After the device release etching process is done, the pulling strings balance the bending torque of the bending bimorphs and stop the mirror frame at about 45°, as shown in Figure 6(a). Then the pulling strings are cut using a sharp-tip tweezer. After that, the bending bimorphs bend the mirror frame towards 100°. Some of the mirror frame bars fall into the notch automatically. If not, the tweezer is used to drag the pulling strings and guide the mirror frame bar to fit into the latch. Figure 6(b) illustrates this process.

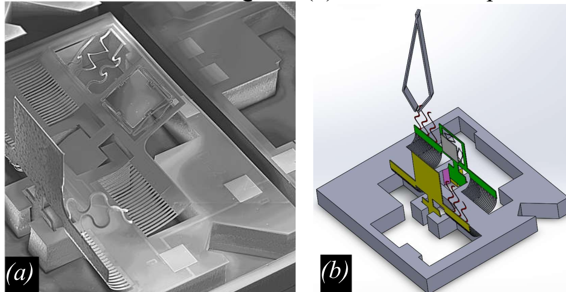

Figure 6. (a) A released device is with the pulling strings for Mirror I cut and those for Mirror II remaining. (b) Cut all the strings and pull them to guide the mirror frame bar into the latch.

Figure 7 shows some SEMs of fabricated devices. The detail of the latch structure is shown in Figure 7(c).

MEMS CHARACTERIZATIONS

MEMS mirror verticality: To evaluate the new latch structure, the bending angles of 10 vertical mirrors from this work and 21 vertical micromirrors from the previous [10] with the simple stopper structure are measured. The bending angle is the angle of a mirror frame measured from its initial flat position. The statistical results are listed in Table 1. The orientation angles of the 10 new vertical micromirrors range from 90° to 95.8° with a standard deviation of 2.1°, which are much improved from the range of 63° to 99° and the standard deviation of 10.5° of the previous designs.

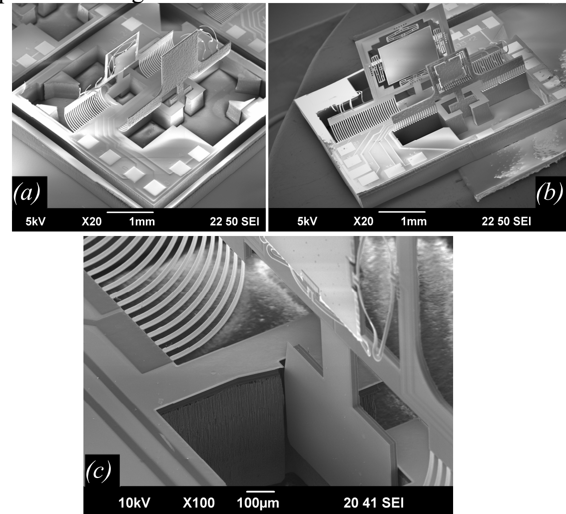

Figure 7. The SEM of the fabricated device after released and guide the mirror frame bar into the stop-and-latch. (a) The forward scanner with a scanning mirror and a fixed mirror. (b) The forward scanner with two scanning mirrors of different sizes. (c) A zoom-in image of the mirror frame bar inside the latch structure.

Table 1: The statistic of the bending angle of the devices from previous works and this work.

	No. of devices	Min.	Max.	Std. Dev.	Absolute Error (AE) to 90°
Previous devices	21	63.0°	99.0°	10.5°	9.5°
This work	10	90.0°	95.8°	2.1°	2.0°

Quasi-static response and frequency response: The measured quasi-static scanning angles of a vertical micromirror are plotted in Figure 8(a), where their maximum optical scanning FoVs are 20°(h) × 22°(v). The measured frequency response is shown in Figure 8(b). The first mode is the mirror frame rotation mode at 0.63 kHz, improved from 0.38 kHz of the previous design due to the adoption of the new latch structure. The second mode is the tip-tilt scanning mode at 1.28 kHz.

Mirror frame rotation: The frame rotation is an unwanted response. The bending bimorph array conducts the electrical current to the vertical micromirror and thus draws Joule heating that tends to cause the mirror frame to rotate upward. However, with the new latch structure in place, the mirror frame bar is latched inside the notch, so the rotation of the mirror frame is constrained. As shown in Table 2, the maximum frame rotation angle of this new design is reduced down to 0.05° from 0.58° of the previous design.

MEMS LiDAR setup and experiment: Figure 9 shows the MEMS LiDAR setup built with the forward-view MEMS laser scanner. It can be seen that the laser beam is scanned forward. The raster scanning pattern (the inset in Figure 9) is achieved with the MEMS mirror actuated at 1 Hz in the X-axis and 10 Hz in the Y-axis. Figure 10(a) shows the

point cloud of a cross-shaped object generated by this MEMS LiDAR. The object is shown in Figure 10(b), which is 13.5 cm away from the LiDAR. The LiDAR point cloud shows a minimal distinguishable distance of 2 cm.

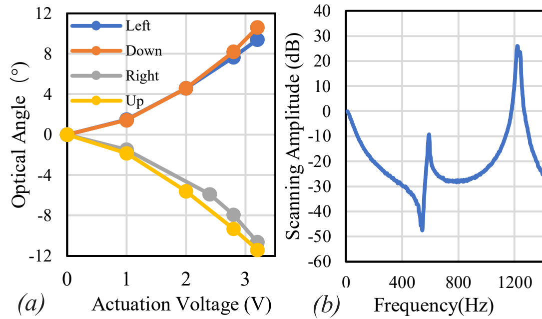

Figure 8. (a) The quasi-static responses of the MEMS mirrors. (b) The frequency response of the MEMS mirror and mirror frame.

Table 2: The comparison of the frame rotation and the resonant frequency of the frame rotation mode.

	Maximum frame rotation during mirror actuation	Resonant frequency of the frame rotation mode
This work	0.05°	0.63 kHz
Previous work	0.58°	0.38 kHz

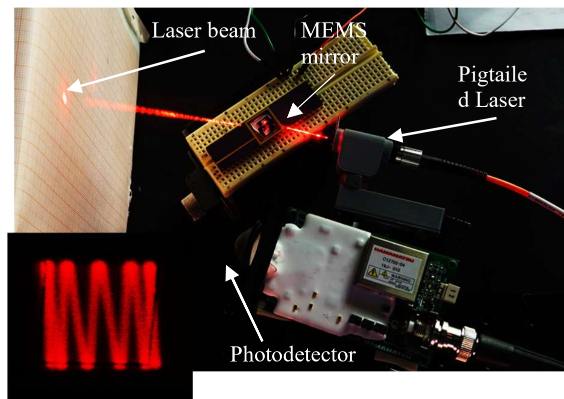

Figure 9. The setup of the forward scanning LiDAR. Inset: Picture of a laser raster scanning pattern.

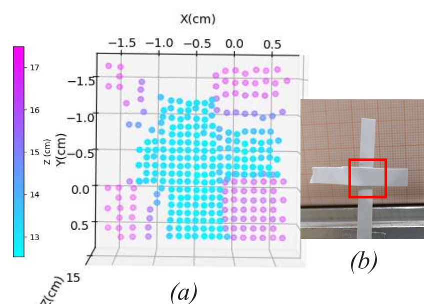

Figure 10. (a) The point cloud generated by the LiDAR with the forward scanning MEMS scanner. (b) The scanning area on the target object.

CONCLUSION

In this work, a forward-view MEMS scanner with a latch structure to improve the verticality of the upright micromirrors is designed and fabricated. Compared to the previous designs, the latch structure can latch the mirror frame to secure the bending angles of both vertical micromirrors. Pulling strings are also designed on the mirror frame so that we can drag the pulling strings to direct the mirror frame into the latch structure. With the new latch structure, the forward-view scanner design shows much-improved verticality in both static and dynamic scanning states. The stiffness is also improved by 1.7 times, making the micromirrors more robust. A forward-view scanning MEMS LiDAR has been built with this MEMS scanner and the acquired point clouds yield a distance measurement accuracy of 2 cm.

ACKNOWLEDGEMENTS

This work is supported by the US Office of Naval Research under the award #N00014-18-1-2663 and the NSF MIST Center.

REFERENCES

[1] R. Halterman, et al., "Velodyne HDL-64E lidar for unmanned surface vehicle obstacle detection", in *Unmanned Systems Technology XII* (Vol. 7692, p. 76920D). SPIE.

[2] A. Kasturi, et al. "UAV-borne lidar with MEMS mirror-based scanning capability", in *Laser Radar Technology and Applications XXI*. (Vol. 9832.) SPIE, 2016.

[3] U. Hofmann, et al. "Biaxial resonant 7mm-MEMS mirror for automotive LIDAR application", in *OMN 2012*. IEEE.

[4] L. Ye, et al. "Large-Aperture kHz Operating Frequency It-alloy Based Optical Micro Scanning Mirror for LiDAR Application", *Micromachines*, 8(4), 120.

[5] G. Perimysium, et al. "External Electromagnet FPCB Micromirror for Large Angle Laser Scanning", Micromachines, 10(10), 667.

[6] K. Jia, et al. "An electrothermal tip–tilt–piston micromirror based on folded dual S-shaped bimorphs", *J. Microelectrodes'. Syst.*, 18.5, pp. 1004-1015, 2019.

[7] D. Wang, et al. "A low-voltage, low-current, digital-driven MEMS mirror for low-power LiDAR", *IEEE Sensors Letters*, 4(8), pp.1-4, 2020.

[8] T. Baisch, et al. "Design and fabrication of the Harvard ambulatory micro-robot", in *Robotics Research*, pp. 715-730, Springer, Berlin, Heidelberg.

[9] R. Wood, et. al. "Flight of the robobees", *Scientific American*, 308(3), 60-65.

[10] D. Wang, et al. "A silicon optical bench with vertically-oriented micromirrors for active beam steering", *Sensors and Actuators A: Physical*, 298, 111586.

CONTACT

*H. Xie, tel: +1-352-283-4162; hk.xie@ieee.org.